PROCEEDINGS OF THE ROYAL SOCIETY B

Proc. R. Soc. B (2008) **275**, 11–17
doi:10.1098/rspb.2007.1188
Published online 17 October 2007

Geometry and self-righting of turtles

Gábor Domokos[1,2] **and Péter L. Várkonyi**[1,*]

[1]*Department of Mechanics, Materials and Structures and* [2]*Center for Applied Mathematics and Computational Physics, Budapest University of Technology and Economics, Muegyetem rkp. 3, K242, Budapest 1111, Hungary*

Terrestrial animals with rigid shells face imminent danger when turned upside down. A rich variety of righting strategies of beetle and turtle species have been described, but the exact role of the shell's geometry in righting is so far unknown. These strategies are often based on active mechanisms, e.g. most beetles self-right via motion of their legs or wings; flat, aquatic turtles use their muscular neck to flip back. On the other hand, highly domed, terrestrial turtles with short limbs and necks have virtually no active control: here shape itself may serve as a fundamental tool. Based on field data gathered on a broad spectrum of aquatic and terrestrial turtle species we develop a geometric model of the shell. Inspired by recent mathematical results, we demonstrate that a simple mechanical classification of the model is closely linked to the animals' righting strategy. Specifically, we show that the exact geometry of highly domed terrestrial species is close to optimal for self-righting, and the shell's shape is the predominant factor of their ability to flip back. Our study illustrates how evolution solved a far-from-trivial geometrical problem and equipped some turtles with monostatic shells: beautiful forms, which rarely appear in nature otherwise.

Keywords: shell morphology; self-righting; monostatic body; static equilibrium

1. INTRODUCTION

The ability of self-righting is crucial for animals with hard shells (Frantsevich & Mokrushov 1980; Faisal & Matheson 2001; Frantsevich 2004; Uhrin *et al.* 2005), e.g. beetles and turtles. It is often used as a measure of individual fitness (Burger *et al.* 1998; Steyermark & Spotila 2001; Ashmore & Janzen 2003; Freedberg *et al.* 2004), although it is also influenced by the environment, e.g. temperature (Elnitsky & Claussen 2006). Both righting behaviour (Ashe 1970; Wassersug & Izumi-Kurotani 1993; Rivera *et al.* 2004; Stancher *et al.* 2006) and the evolution of shell morphology (Rouault & Blanc 1978; Claude *et al.* 2003; Myers *et al.* 2006) of turtles have been studied recently. An example of their interaction is the sexual dimorphism of species where males are often overturned during combats (Bonnet *et al.* 2001; Willemsen & Hailey 2003; Mann *et al.* 2006), and their shell has adapted to facilitate righting. Here we develop a geometric shell model based on field data to uncover systematically the connections between righting strategies and turtle shell morphology.

Righting is always performed via a transversal roll around the turtle's longitudinal axis, along the perimeter of the 'main' transversal cross-section at the middle of the body. Thus, the roll's geometry is essentially *planar* and can be readily illustrated (figure 1), suggesting a planar model: a convex, homogeneous disc rolling under gravity on a horizontal surface. Although turtles are neither exactly convex nor exactly homogeneous, these seem to be plausible first approximations. The difficulty of righting originates in the 'potential hill' (represented by the unstable equilibrium at the side); the turtle has to produce biomechanical energy to overcome this obstacle. An obvious question is whether a contour *without this obstacle* exists; such a hypothetical shape would have just one stable and one unstable equilibrium point and, according to the planar model, turtles with this contour could perform righting effortlessly. Nevertheless, one can prove (Domokos *et al.* 1994) that each homogeneous, convex disc has at least two stable equilibria (like an ellipse). This appears to be bad news for turtles. However, as we are about to show, the planar model proves to be an oversimplified approach.

Although the *geometry* of the roll can be illustrated in two dimensions, the *mechanics* is fundamentally three dimensional: the centre of gravity G is determined not just by the main cross-section but by the complete body. For example, in a long, solid cylinder with ends chopped off diagonally in opposite directions, G is off-centre from the longitudinal axis of the cylinder, and thus the cylinder tends to self-right. V. I. Arnold suggested (Domokos 2006) that, in contrast to planar discs, convex, homogenous three-dimensional objects with just *one stable* and *one unstable* equilibrium may exist. The conjecture turned out to be correct and led to the classification of three-dimensional bodies with respect to the number of stable and unstable equilibria (Várkonyi & Domokos 2006*a*,*b*). Here we apply a simplified classification, referring only to *stable* balance points (*unstable* ones are less relevant for turtles). Stability class S_i ($i=1, 2, 3, \ldots$) contains all objects with i stable equilibria when resting on a horizontal surface. Of particular interest are objects in class S_1 also called *monostatic* (Conway & Guy 1969; Dawson & Finbow 1999). Turtles in S_1 can self-right without any effort. Monostatic bodies are rare in nature: systematic experiments with 2000 pebbles identified no such object (Várkonyi & Domokos 2006*a*). Even rarer are monostatic bodies with two equilibria altogether (satisfying Arnold's above-mentioned conjecture); nevertheless, the shape of

* Author for correspondence (vpeter@mit.bme.hu).

Electronic supplementary material is available at http://dx.doi.org/10.1098/rspb.2007.1188 or via http://journals.royalsociety.org.

Received 30 August 2007
Accepted 21 September 2007

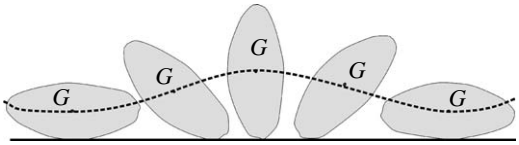

Figure 1. Rigid disc (representing the main transversal section of the turtle shell) rolling on a horizontal line. The thick dashed line denotes the orbit of the centre of gravity (G) during rolling. The peaks/valleys of the orbit correspond to local extrema of the potential energy, i.e. unstable/stable equilibria of the rigid body. For convex, homogenous two-dimensional discs, there are always at least two stable points (Domokos *et al.* 1994).

some highly domed terrestrial turtles is strongly reminiscent of them (Várkonyi & Domokos 2006*b*).

The goal of this paper is to identify equilibrium classes S_i of real turtles and the relation of these equilibrium classes to righting behaviour. In particular, we are interested in whether monostatic shell shapes exist or not. We develop a simple geometric model of the shell, and fit model parameters to real measured shapes. The equilibrium class of the fitted model is numerically determined and compared with known data about the righting behaviour of turtles.

2. METHODS: THE GEOMETRIC SHELL MODEL

Here we summarize the construction of the shell model in three steps (transversal, longitudinal and three-dimensional models). We also describe the method of fitting the model parameters to individual measured turtle shapes, and the technique to determine the equilibrium class of the three-dimensional model.

In the shell model (figure 2), a planar curve represents the approximate transversal contour of the shell (*transversal model*, see figure 2*a*). This curve has three parameters (figure 3): p, controlling the shape of the carapace; R, defining the height/width ratio of the contour (or alternatively the *relative positions* of the carapace and the plastron); and k, determining the transition between plastron and carapace.

The transversal model (figure 2*a*) is constructed in a polar coordinate system, with origin at the middle of the contour, both horizontally and vertically. Height and width of the cross-section are scaled to $2R$ and 2, respectively. The contour K of the cross-section is achieved from the curves of the plastron (P) and the carapace (C). The plastron is approximated by a straight line given in our polar coordinate system by

$$P(\alpha, R, k) = \begin{cases} p_0/\cos\alpha & \text{if} \quad -\pi/2 \le \alpha \le \pi/2 \\ \text{(not defined otherwise)} & \end{cases}, \tag{2.1}$$

where p_0 is a scaling factor. The shape of the carapace is first approximated in an orthogonal u–v coordinate system by the curve (figure 2*b*)

$$u = \pm(-v - pv^2)^{1/2}. \tag{2.2}$$

This curve is either an ellipse ($p>0$) or a hyperbola ($p<0$). Next, the curve is expressed in the polar coordinate system of figure 2*a* by substituting

$$u = c_0 C \sin\alpha, \tag{2.3}$$

$$v = -c_0[C\cos\alpha + R], \tag{2.4}$$

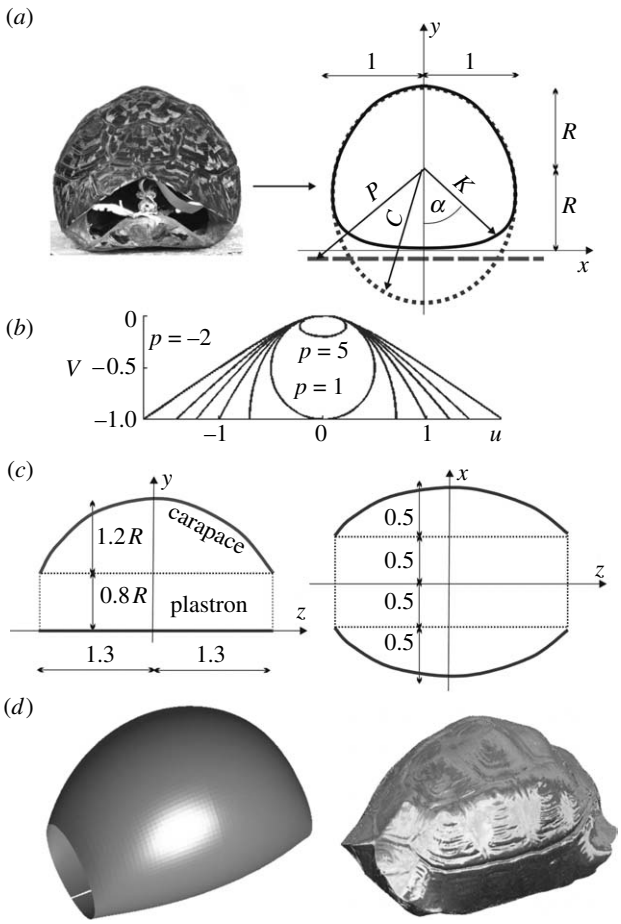

Figure 2. Turtle shell model. (*a*) Frontal view of shell (*Stigmochelys pardalis*) and three-parameter transversal model K (α, R, p, k) of main cross-section. The plastron is approximated by straight line P (equation (2.1)). The carapace is approximated by curve C (equations (2.2)–(2.4)); smooth transition between plastron and carapace achieved by merging function (equation (2.5)). (*b*) Carapace shape at various values of parameter p. (*c*) Longitudinal model: schematic side- and top-view contours are circular arcs obtained as averages from measurements; sizes are normalized. (*d*) Visual comparison of digitized shell image and model surface.

into (2.2) and solving it for C; c_0 is again a scaling factor. The final contour $K(\alpha, R, p, k)$ is constructed as

$$K = [C^{1/k} + P^{1/k}]^k, \tag{2.5}$$

where the negative parameter $0>k>-1$ determines the roundedness of the transition between the plastron and the carapace. The factors c_0 and p_0 are determined numerically from the respective constraints that the lowest point of the final contour is at distance R and the widest points are at distance 1 from the origin of the polar coordinate system. The highest point of the carapace is automatically at distance R above the origin (since the point $(u, v)=(0, 0)$ of the curve corresponds to $(C, \alpha)=(R, \pi)$, cf. (2.3) and (2.4)). At some values of α, the curves P (for $\pi/2<\alpha\le 3\pi/2$) and C (in an interval around $\alpha=0$ if $p<0$) are not defined. Here (2.5) is replaced by $K\equiv C$ and $K\equiv P$, respectively.

Contours (cf. figure 2*a*) of 30 turtles belonging to 17 species have been digitized and the three parameters p, R and k of the transversal model were fitted to these contours by considering $n\approx 1000$ equidistant angles $\alpha_i=2i\pi/n$ ($i=1, 2, \ldots, n$) in our polar coordinate system and by minimizing

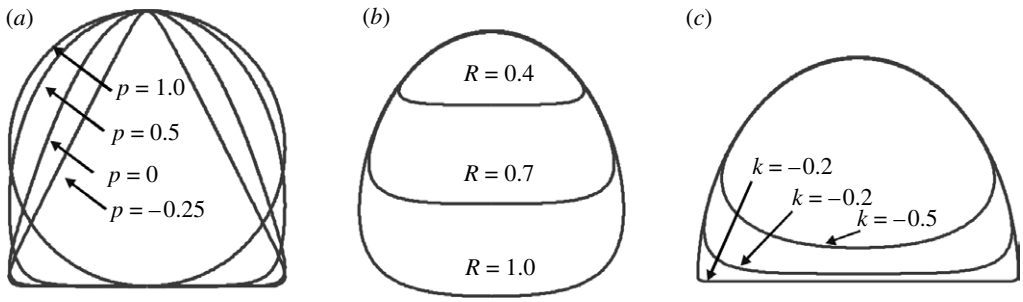

Figure 3. Main cross-sections at various parameter values. (*a*) Parameter p determines the shape of the carapace ($R=1$, $k=-0.1$), (*b*) R determines the relative positions of the carapace and the plastron ($p=0.5$, $k=-0.25$) and (*c*) k determines the roundedness at the carapace–plastron transition ($R=0.7$, $p=0.5$).

the mean square radial error

$$e=\sqrt{\frac{1}{n}\sum_i [K(\alpha_i)-Q(\alpha_i)]^2}. \tag{2.6}$$

Here $K(\alpha_i)$ and $Q(\alpha_i)$ denote points of the model and the measured contour, respectively. The results of the parameter fitting are summarized in the electronic supplementary material, table 1. Electronic supplementary material, figure 7 compares the measured contours to optimally fitted model contours.

The *longitudinal* model describing side- and top-view contours of the shell (figure 2*c*) has been constructed using averaged data from the above-mentioned 30 individuals. Needless to say, the circular and straight contours and the parameter values of figure 2*c* do not represent a precise fit to real animals. However, the mechanical behaviour is much less sensitive to these curves than to the shape of the transversal model: turtles *always* roll transversally along the perimeter of the main cross-section. The only significant effect of the longitudinal model is to modify the height of the centre of gravity. Slightly modified longitudinal curves have been tested and showed identical qualitative behaviour.

Finally, the *three-dimensional model surface* emerges as a series of horizontally and vertically scaled versions of the main transversal section, fitting the longitudinal contours (figure 2*d* and electronic supplementary material, figure 8).

To determine the equilibrium class of the model at given values of p, R and k, the centre of gravity G of the model was integrated numerically (due to the two planes of reflection symmetry, only the y-coordinate of G needs to be computed). Equilibrium points of the three-dimensional model surface can be conveniently identified by considering the radius ρ pointing from the centre of gravity G to the model surface, as a scalar function of two coordinates, e.g. α and z (cf. figure 2*a*,*c*). As it was shown in Domokos *et al.* (1994) mechanical equilibria coincide with stationary points of $\rho(\alpha, z)$, i.e. points where the gradient vector $\left[\partial\rho/\partial\alpha \quad \partial\rho/\partial z\right]$ is zero. Specifically, stable equilibria occur at local minima of $\rho(\alpha, z)$, unstable equilibria occur at saddle points and local maxima. All these stationary points can be readily computed for the given, three-dimensional model surface $\rho(\alpha, z)$ with fitted p, R and k parameter values; the equilibrium class S_i is identified simply by counting the minima.

Our three-dimensional model leaves the rostral and caudal ends of the shell undefined; we assume that the turtle has only unstable equilibrium points in these domains, in accordance with the facts that the real shells are somewhat elongated and turtles do not tend to get stuck in head- or tail-down positions.

3. RESULTS: EQUILIBRIUM CLASSES, ENERGY BALANCE AND RIGHTING STRATEGIES

The previously described procedure identifies the fitted shape parameters R, p and k corresponding to any shell and the complete algorithm to determine the equilibrium class of any *individual turtle* (as given in the electronic supplementary material, table 1). In order to analyse *global trends*, we introduce simplified, lower dimensional (two parameter and one parameter) models, trading accuracy of individual predictions for visual and conceptual simplicity.

As a first step we eliminate parameter k. We consider the $[R, k]$ projection of the $[R, p, k]$ space (figure 4*a*). Measured turtles are marked by squares; two dashed lines $k^+(R)$ and $k^-(R)$ mark the approximate upper and lower envelopes of the data points. Figure 4*b* shows the $[R, p]$ projection of the $[R, p, k]$ space. In addition to marking the measured turtles, we also determined the equilibrium class of each $[R, p]$ point by assuming for k the extreme values $k=k^+(R)$ and $k=k^-(R)$. Dashed lines depict the boundaries between equilibrium classes S_1, S_2 and S_3 for both cases. As we can observe in figure 4*b*, not even these extreme changes of k have substantial influence on the borders. Few marks appear in the ambiguous grey zone between the two sets of boundaries; the equilibrium class of the overwhelming majority of individual turtles is unambiguously determined by the simplified, two-parameter $[R, p]$ model, yielding the following observations:

(i) although class S_1 is represented by a rather small domain (small ranges both for R and p), nevertheless, tall turtles are remarkably close to S_1, i.e. they tend to be *monostatic* and
(ii) flat turtles fall into S_2, the majority of medium turtles falls into S_3.

Next, we further simplify our model to better understand global trends: strong linear correlation between the parameters ($\mathrm{corr}\langle R, p\rangle=0.73$; $\mathrm{corr}\langle R, k\rangle=0.64$) suggests that a one-parameter (R) model family is sufficient to approximate the geometry. From the biological point of view, this implies that a single, visually significant parameter (the height/width ratio R) basically determines, as we will see soon, the righting strategy. Figure 4*c* illustrates the angular location of equilibria as R is varied in this one-parameter model and reveals a classical pitchfork bifurcation. This simple one-parameter model illustrates the transition between three different types of turtles:

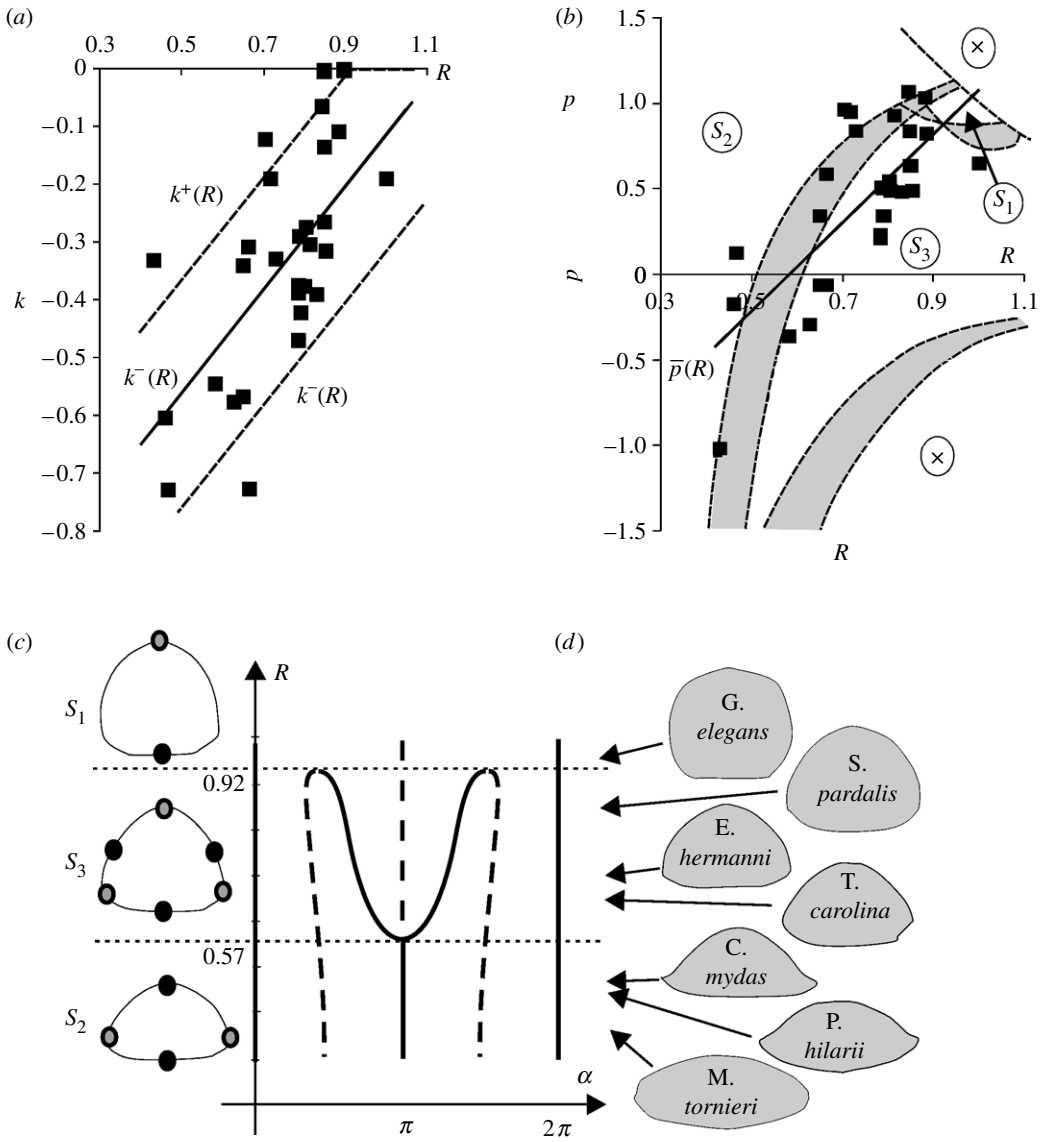

Figure 4. Measured turtles and equilibrium classes. (*a*,*b*) Squares show the fitted model parameters corresponding to individual turtles in the $[R, k]$ and $[R, p]$ parameter planes. Linear regression (continuous lines) reveals $\bar{k}(R) = 0.90R - 1.01$ and $\bar{p}(R) = 2.59R - 1.51$. (*a*) Dashed lines $k^{\pm}(R) = \min(0, \bar{k}(R) \pm 0.2)$ mark the approximate upper and lower envelope of the data points. (*b*) The equilibrium class of the model was determined for each point of the parameter space $[R, p]$ under the assumptions of $k = k^{+}(R)$ and $k = k^{-}(R)$; boundaries of classes S_1, S_2 and S_3 are shown by dashed lines in both cases. The grey shading between the two sets of boundaries shows regions of the $[R, p]$ space where the equilibrium class of an individual may depend on k. Domain 'X' corresponds to parameter values not compatible with the model. (*c*) Angular positions α of equilibria on the main cross-section of the turtle shell as function of R under assumptions of $k = \bar{k}(R)$ and $p = \bar{p}(R)$. Equilibria in all classes marked on main transversal cross-section by black (stable) and grey (saddle point) circles. Unstable equilibria off the main cross-section (near head and tail) are not indicated. (*d*) Fitted R value and contour of some measured individuals.

(i) flat individuals tend to have two stable equilibria, one on the plastron and one opposite, on the carapace,
(ii) as R increases, two additional stable equilibria emerge on the back and their distance grows monotonically, and
(iii) the additional stable equilibria vanish for high R values, here monostatic turtles appear.

A closer look at an actual shell (figure 2*d*) explains why monostatic bodies may exist in three dimensions in contrast to two dimensions: the front and back parts of the shell are lower than the main cross-section, thus the centre of gravity G of a complete turtle body is closer to the plastron than the centre of its main cross-section. The lower position of G makes self-righting easier than predicted by the planar model of §1. While this simple qualitative observation is intuitively helpful, it certainly does not account for the *quantitative* agreement between model parameters of highly domed turtle shells and monostatic bodies (cf. figure 4*b*; electronic supplementary material, table 1).

The *energy balance* of righting on a horizontal surface reveals a close relationship between the equilibrium class and the righting strategy (for the latter, see Ashe 1970 and Rivera *et al.* 2004). Non-monostatic turtles have to overcome a primary potential barrier (*primary energy deficit* D_p, figure 5*a*) due to the unstable equilibrium at the turtle's side. Additionally, secondary deficit (D_s) results from shell imperfections (figure 5*a*). Turtles with high energy barriers use primarily their necks for righting (Rivera *et al.* 2004), thus the *excess neck length* N (figure 5*b*)

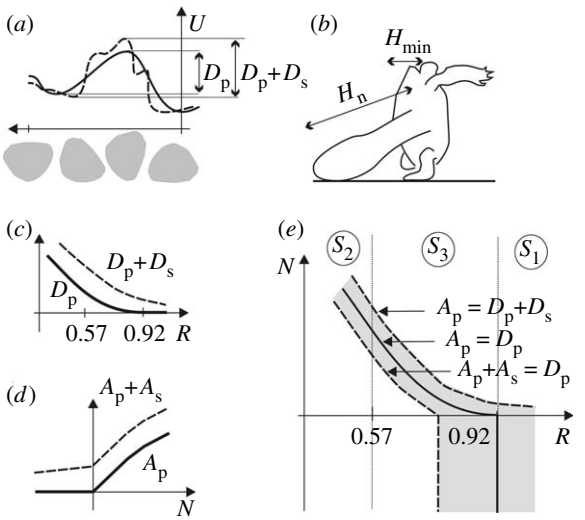

Figure 5. Energy balance of righting. (*a*) Illustration of primary (D_p) and secondary (D_s) energy deficit of rolling turtle due to potential energy barrier between stable equilibria. Continuous/dashed line denotes potential energy U of perfect/imperfect shell normalized by body size. (*b*) Schematic frontal view of a righting turtle. The neck's excess length is defined as $N=(H_n-H_{min})/H_{min}$, i.e. scaled difference between the neck's length (H_n) and the distance (H_{min}) from the neck's base to the top of the carapace. (*c*) Primary (D_p) and secondary (D_s) energy deficit as functions of R. $D_p(R)$ is decreasing and vanishes for monostatic ($R>0.92$) turtles. (*d*) Available biomechanical energy as function of the excess neck length N: primary (A_p) due to excess neck length N ($A_p=0$ for $N<0$; $A_p(N)$ increasing for $N>0$), secondary (A_s) due to dynamical effects, head and limb bobbing, horizontal push by leg, etc. (*e*) Energy balance curves in the $[R, N]$ plane. In the grey region, secondary components (D_s, A_s) determine righting success. To the right of the grey region, righting is successful even in the presence of secondary deficits (shell irregularities). To the left, righting is unsuccessful even if secondary available energy (from head-bobbing, etc.) is used. Observe characteristic behaviour in the three principal equilibrium classes: narrow grey band in S_2, wide region in S_1 and mixed in S_3.

is the dominant factor of *primary available* biomechanical energy (A_p). Additionally, secondary energy (A_s) is generated by limb- and head bobbing, ventral orientation of the head or feet (to move centre of gravity), and nearly horizontal pushing with the legs (using friction; Ashe 1970). The latter often results in rotation around a vertical axis during righting efforts, helping the feet find support.

Here we perform a qualitative, theoretical analysis of the energy balance based on two simple assumptions: $D_p(R)$ decreases monotonically with R and vanishes for monostatic (S_1) turtles (figure 5*c*); $A_p(N)$ increases monotonically with N if $N>0$ and $A_p=0$ for $N\leq 0$ (figure 5*d*).

Energy balance curves, i.e. solutions of $A_p(+A_s)=D_p(+D_s)$ can be plotted in the plane of geometric parameters R and N (figure 5*e*). Turtles represented by points to the *right* of the curves stand a good chance of righting themselves. Turtles to the *left* of the curves are expected to have serious difficulty. Our assumptions lead to the following *qualitative* conclusions:

(i) For flat turtles (R under approx. 0.6, figure 6*a*) inside S_2, the curves form a *narrow band*, indicating that the primary parameters R and N dominate

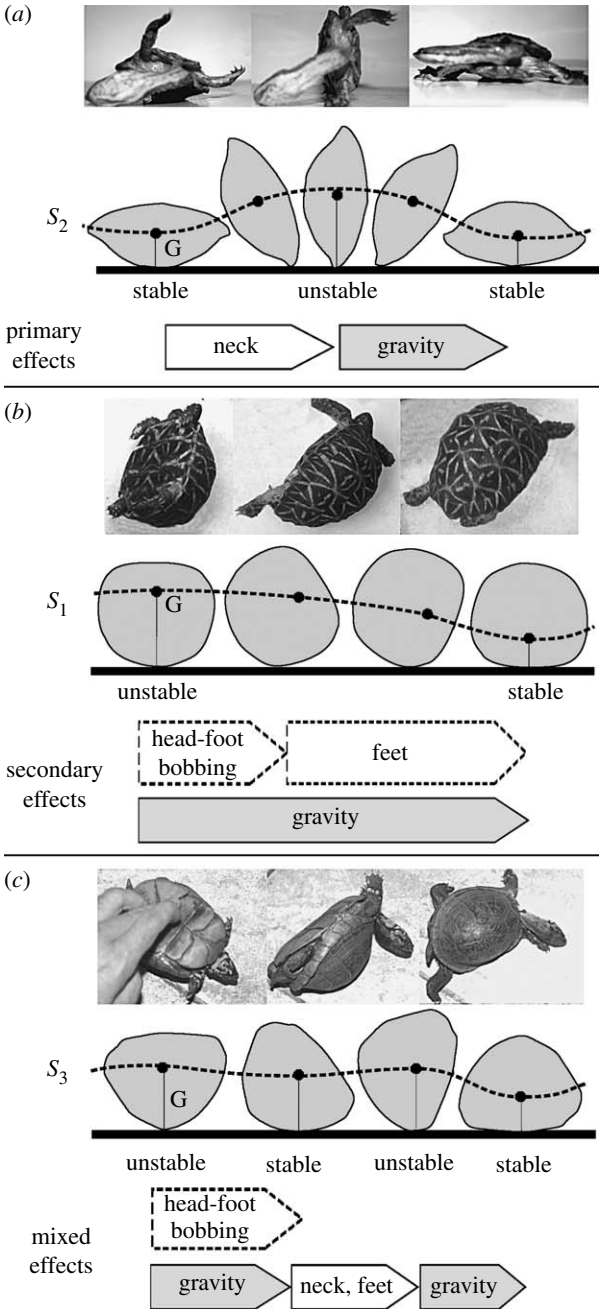

Figure 6. Righting strategies. Each strategy is characterized by the typical shape of the rolling main cross-section (grey contours) as well as the orbit (dashed line) of the centre of gravity G. Arrows denote key elements of righting, dashed arrows apply in presence of secondary energy barriers. (*a*) Flat turtles ($R<\sim 0.6$ inside class S_2, photo: *Hydromedusa tectifera*): high primary energy barrier between stable and unstable equilibria is overcome by primary biomechanical energy resulting from vertical push with neck. Righting fitness is determined by primary geometric parameters (height/width ratio R, excess neck length N). (*b*) Tall turtles ($R>\sim 0.8$, inside or close to monostatic class S_1, photo: *Geochelone elegans*): small, secondary energy barriers (resulting mainly from shell imperfections) are overcome by secondary sources of biomechanical energy: head- and foot-bobbing, push by feet. (*c*) Medium turtles ($\sim 0.6<R<0.8$, inside or close to class S_3, photo: *Terrapene carolina*): in the first phase of roll, secondary barriers are overcome by dynamic (secondary) energy; in the second phase, the primary energy barrier is overcome by primary energy (push with neck, feet).

righting fitness. The *associated righting strategy* is based on primary energies: righting is accomplished via a strong vertical push with the neck and lifting the turtle sufficiently to overcome the primary energy barrier. Most aquatic and semi-aquatic turtles, e.g. side-necked turtles (Pleurodira), snapping turtles (Chelydridae), mud turtles (Kinosternidae) follow this strategy:

(ii) Tall turtles (R above approx. 0.8, figure 6*b*) inside or close to the monostatic class S_1, usually have shorter necks than their carapace heights, i.e. $N<0$. Thus, their R and N values are in the *wide grey zone* between the curves of figure 5*e*, indicating the dominance of secondary effects in righting fitness. The *associated righting strategy* is based on secondary energies: righting either starts spontaneously (Ashe 1970) or it is accomplished by dynamic motion of the limbs, to overcome small shell imperfections. Subsequently, when the plastron is already close to vertical and the legs reach the surface, horizontal pushing with the legs (using friction) produces additional moments to overcome secondary energy barriers. This is the primary strategy of highly domed terrestrial tortoises with short necks and rounded cross-sections, such as *Geochelone*, *Stigmochelys*, *Astrochelys*, and some *Terrapene* and *Testudo* species.

(iii) For medium turtles ($\sim 0.6<R<\sim 0.8$, figure 6*c*), in or close to S_3, the energy diagram shows regions of both types: the three curves initially form a narrow band and subsequently diverge. The *associated righting strategy* is composed as a *mixture* of the previous two: if placed on the middle of the back, the turtle starts rolling spontaneously, assisted by dynamic limb and head motion to overcome shell irregularities (similar to class S_1) until it reaches stable equilibrium. From there, the successful righting strategy is based on a vertical push with the neck (similar to class S_2), accompanied by pushing with the legs. Many tortoises (e.g. *Psammobates*, many *Testudo* and *Terrapene* species) belong to this group.

Due to the strong correlation between model parameters, by measuring the R=height/width ratio one can often correctly predict the righting strategy (figure 4*b*,*d*). *Quantitative* analysis of the individual's energy balance would require more detail about the neck, the shell imperfections and other ingredients.

4. DISCUSSION

Many factors have been identified that affect the shape of turtles. Flat shells with sharp and smooth edges are advantageous, respectively, for swimming (Claude *et al.* 2003), and for digging (Willemsen & Hailey 2003). On the other hand, *increased shell height* was found to offer better protection against the snapping jaws of predators (Pritchard 1979); it also protects from desiccation and improves thermoregulation (Carr 1952). While these factors indicate qualitatively that higher shells might be of advantage, they can neither be applied for quantitative prediction, nor do they determine the optimal height/width ratio. Our study is much more specific: it not only shows that there exists a narrow optimal (monostatic) range of the height/width ratio for self-righting in a terrestrial environment, but also predicts the exact optimal geometry.

The height/width ratio of highly domed species (*Geochelone elegans*, *Geochelone radiata*) is near the minimum for monostatic shapes ($R\approx 0.9$), indicating an optimal trade-off between self-righting ability and other factors penalizing increased height (e.g. decreased stability). The shape parameter p is also in the optimal range for these species ($0.8<p<1.1$). Thus, the advantage of being close to monostatic not only determines the height/width ratio, but the exact shape (e.g. roundedness).

It would be worth exploring how other morphological differences between aquatic and terrestrial turtles (Acuna-Mesen 1994; Mann *et al.* 2006) affect their righting fitness. Another observation of particular interest is that bad nourishment often produces shell imperfections (Highfield 1989; Wiesner & Iben 2003), decreasing the chances of successful righting, according to the presented theory.

The experiments comply with all relevant local and institutional guidelines.

This research was supported by OTKA grant T72146 and the Zoltán Magyari Postdoctoral Fellowship. We thank Gyula Hack, Doma Csabay, Mrs József Bíró, Diana Cseke, Judit Vörös, Zoltán Korsós and Timea Szabó for providing access to turtles. Comments from John Iverson, Géza Meszéna, István Scheuring, Patrick Simen and Andy Ruina as well as from anonymous referees are appreciated.

REFERENCES

Acuna-Mesen, R. A. 1994 Morphometric variation and ecologic characteristics of the habitat of the *Kinosternon scorpioides* turtle in Costa Rica (Chelonia, Kinosternidae). *Rev. Bras. Biol.* **54**, 537–547. [In Portuguese.]

Ashe, V. M. 1970 The righting reflex in turtles: a description and comparison. *Psychon. Sci.* **20**, 150–152.

Ashmore, G. M. & Janzen, F. 2003 Phenotypic variation in smooth softshell turtles (*Apalone mutica*) from eggs incubated in constant versus fluctuating temperatures. *Oecologia* **134**, 182–188.

Bonnet, X. *et al.* 2001 Sexual dimorphism in steppe tortoises (*Testudo horsfieldii*): influence of the environment and sexual selection on body shape and mobility. *Biol. J. Linn. Soc.* **72**, 357–372. (doi:10.1006/bijl.2000.0504)

Burger, J., Carruth-Hinchey, C., Ondroff, J., McMahon, M., Gibbons, J. W. & Gochfeld, M. 1998 Effects of lead on behaviour, growth, and survival of hatchling slider turtles. *J. Toxicol. Environ. Health A* **55**, 495–502. (doi:10.1080/009841098158296)

Carr, A. F. 1952 *Handbook of turtles. The turtles of the United States, Canada, and Baja California*. Ithaca, NY: Cornell University Press.

Claude, J., Paradis, E., Tong, H. & Auffray, J.-C. 2003 A geometric morphometric assessment of the effects of environment and cladogenesis on the evolution of the turtle shell. *Biol. J. Linn. Soc.* **79**, 485–501. (doi:10.1046/j.1095-8312.2003.00198.x)

Conway, J. & Guy, R. 1969 Stability of polyhedra. *SIAM Rev.* **11**, 78–82. (doi:10.1137/1011014)

Dawson, R. & Finbow, W. 1999 What shape is a loaded die? *Math. Intelligencer* **22**, 32–37.

Domokos, G. 2006 My lunch with Arnold. *Math. Intelligencer* **28**, 31–33.

Domokos, G., Papadopoulos, J. & Ruina, A. 1994 Static equilibria of planar, rigid bodies: is there anything new? *J. Elasticity* **36**, 59–66. (doi:10.1007/BF00042491)

Elnitsky, M. A. & Claussen, D. L. 2006 The effects of temperature and inter-individual variation on the locomotor performance of juvenile turtles. *J. Comp. Physiol. B* **176**, 497–504. (doi:10.1007/s00360-006-0071-1)

Faisal, A. A. & Matheson, T. 2001 Coordinated righting behaviour in locusts. *J. Exp. Biol.* **204**, 637–648.

Frantsevich, L. 2004 Righting kinematics in beetles (Insecta: Coleoptera). *Arthropod Struct. Dev.* **33**, 221–236. (doi:10.1016/j.asd.2004.05.007)

Frantsevich, L. I. & Mokrushov, P. A. 1980 Turning and righting in geotrupes (Coleoptera, Scarabaeidae). *J. Comp. Physiol.* **136**, 279–289. (doi:10.1007/BF00657348)

Freedberg, S., Stumpf, A. L., Ewert, M. A. & Nelson, C. E. 2004 Developmental environment has long-lasting effects on behavioural performance in two turtles with environmental sex determination. *Evol. Ecol. Res.* **6**, 739–747.

Highfield, A. C. 1989 Notes on dietary constituents for herbivorous terrestrial chelonian and their effects on growth and development. *ASRA (UK) J.* **3**, 7–20.

Mann, G. K. H., O'Riain, M. J. & Hofmeyr, M. D. 2006 Shaping up to fight: sexual selection influences body shape and size in the fighting tortoise (*Chersina angulata*). *J. Zool.* **269**, 373–379. (doi:10.1111/j.1469-7998.2006.00079.x)

Myers, E. M., Janzen, F. J., Adams, D. C. & Tucker, J. K. 2006 Quantitative genetics of plastron shape in slider turtles (*Trachemys scripta*). *Evolution* **60**, 563–572.

Pritchard, P. C. H. 1979 *Encyclopedia of turtles*. Neptune, NJ: TFH Publications.

Rivera, A. R. V., Rivera, G. & Blob, R. W. 2004 Kinematics of the righting response in inverted turtles. *J. Morphol.* **260**, 322.

Rouault, J. & Blanc, C. P. 1978 Notes on the reptiles of Tunisia. V. Biometric characteristics of *Mauremys caspica leprosa* (Schweigger, 1812), in French. *Arch. Inst. Pasteur Tunis.* **55**, 337–357.

Stancher, G., Clara, E., Regolin, L. & Vallortigara, G. 2006 Lateralized righting behaviour in the tortoise (*Testudo hermanni*). *Behav. Brain Res.* **173**, 315–319. (doi:10.1016/j.bbr.2006.06.023)

Steyermark, A. C. & Spotila, J. R. 2001 Maternal identity and egg incubation temperature effects on snapping turtle (*Chelydra serpentina*) righting response. *Copeia* **4**, 1050–1057. (doi:10.1643/0045-8511(2001)001[1050:BTAMIA]2.0.CO;2)

Uhrin, A. V., Slade, C. L. & Holmquist, J. G. 2005 Self righting in the free-living coral *Manicina areolata* (Cnidaria: Scleractinia): morphological constraints. *Caribb. J. Sci.* **41**, 277–282.

Várkonyi, P. L. & Domokos, G. 2006*a* Static equilibria of rigid bodies: dice, pebbles and the Poincaré–Hopf theorem. *J. Nonlin. Sci.* **16**, 255–281. (doi:10.1007/s00332-005-0691-8)

Várkonyi, P. L. & Domokos, G. 2006*b* Mono–monostatic bodies: the answer to Arnold's question. *Math. Intelligencer* **28**, 34–38.

Wassersug, R. & Izumi-Kurotani, A. 1993 The behavioral reactions of a snake and a turtle to abrupt decreases in gravity. *Zool. Sci.* **10**, 505–509.

Wiesner, C. S. & Iben, C. 2003 Influence of environmental humidity and dietary protein on pyramidal growth of carapaces in African spurred tortoises (*Geochelone sulcata*). *J. Anim. Phys. Anim. Nutr.* **87**, 66–74. (doi:10.1046/j.1439-0396.2003.00411.x)

Willemsen, R. E. & Hailey, A. 2003 Sexual dimorphism of body size and shell shape in European tortoises. *J. Zool. Lond.* **260**, 353–365. (doi:10.1017/S0952836903003820)